Analytical asymptotic solutions of $nA+mB \rightarrow C$ reaction-diffusion equations in two-layer systems: A general study

P. M. J. Trevelyan, D. E. Strier,* and A. De Wit

Nonlinear Physical Chemistry Unit, Center for Nonlinear Phenomena and Complex Systems,
Faculté des Sciences, Université Libre de Bruxelles (ULB), CP 231, 1050 Brussels, Belgium
(Received 16 May 2008; published 26 August 2008)

Large time evolution of concentration profiles is studied analytically for reaction-diffusion systems where the reactants A and B are each initially separately contained in two immiscible solutions and react upon contact and transfer across the interface according to a general $nA+mB \rightarrow C$ reaction scheme. This study generalizes to immiscible two-layer systems the large time analytical asymptotic limits of concentrations derived by Koza [J. Stat. Phys. **85**, 179 (1996)] for miscible fluids and for reaction rates of the form $A^n B^m$ with arbitrary diffusion coefficients and homogeneous initial concentrations. In addition to a dependence on the parameters already characterizing the miscible case, the asymptotic concentration profiles in immiscible systems depend now also on the partition coefficients of the chemical species between the two solution layers and on the ratio of diffusion coefficients of a given species in the two fluids. The miscible time scalings are found to remain valid for the immiscible fluids case. However, for immiscible systems, the reaction front speed is enhanced by increasing the stoichiometry of the invading species over that of the species being invaded. The direction of the front propagation is found to depend on the diffusion coefficient of the invading species in its initial fluid but not on its value in the invading fluid. Hence, a reaction front in immiscible fluids can travel in the opposite direction to the reaction front formed in miscible fluids for a range of parameter values. The value of the invading species partition coefficient affects the magnitude of the front speed but it cannot alter the direction of the front. For sufficiently large times, the total amount of product produced in time is independent of the rate of the reaction. The centre of mass of the product can move in the opposite direction to the center of mass of the reaction rate.

I. INTRODUCTION

Simple $A+B \rightarrow C$ chemical reactions are able to generate reaction fronts when two solutions each containing one of the reactants are put in contact. From a chemical engineering perspective, such a reaction is especially useful for extraction purposes because the reaction can help increase the transfer from one phase to the other of a given chemical. In this regard, an evaluation of the efficiency of the extraction technique relies on a good estimate of the temporal evolution of the underlying concentration profiles and of the transfer rate across the interface between the two immiscible solvents.

In this context, recent experiments analyzing the dynamics of concentration profiles in immiscible two-layer systems each containing initially separated reactants have revived interest into the theoretical analysis of the corresponding analytical asymptotic reaction-diffusion profiles. The experiments consist of Hele-Shaw cells (two glass plates separated by a thin gap width) in which two immiscible fluids are put into contact [1–5]. Each layer contains one reactant of a simple $A+B \rightarrow C$ type of reaction. Upon transfer across the interface of one of the reactants (the other one being, in these specific experiments, immiscible in the other layer), a reaction front is formed that invades one of the two layers. Hydrodynamic instabilities driven by buoyancy [1,2,5] and Marangoni effects [3,5] deform the front giving rise to

chemohydrodynamic patterns. From a theoretical point of view, an understanding of the underlying reaction-diffusion base state of the system, where hydrodynamic forces are absent, is of major importance. Indeed such a situation is the starting point for the identification and evaluation of the onset of the instabilities that are present in the full chemohydrodynamic system [6,7].

When analyzing such reaction-diffusion fronts, one of the most important physical quantities is the rate of production $R_c(X,T)$ of the product, with X the dimensional spatial coordinate and T the dimensional time. The position of the reaction front $X_f(T)$ is usually defined as the position where the production rate R_c reaches its maximum [8], however, as pointed out by Cornell *et al.* [9] and Magnin [10] this definition of X_f does not coincide with the asymptotic location where the reactant concentrations vanish when $n \neq m$. Hence, in general it is better to use the definition by Chopard *et al.* [11] in which X_f is the first moment of the production rate, namely,

$$X_f = \frac{\displaystyle\int_{-\infty}^{\infty} R_c X \, dX}{\displaystyle\int_{-\infty}^{\infty} R_c \, dX}, \qquad (1)$$

which is found to coincide with the asymptotic location where the reactant concentrations vanish. A useful measure of the width of the reaction front $W_f(T)$ comes from the

---

*Present address: Roch SA, Av. Madero 1020, Piso 21, C1106ACX, Buenos Aires, Argentina

second moment of the production rate R_c expressed by [9,11,12]

$$W_f^2 = \frac{\int_{-\infty}^{\infty} R_c (X - X_f)^2 dX}{\int_{-\infty}^{\infty} R_c dX}. \tag{2}$$

Such position and width of the reaction front are typical quantities measurable in experiments.

The simplest reaction mechanism between two reactants is $A + B \rightarrow C$ in which the production rate $R_c = kAB$ where k denotes the kinetic constant and A and B denote concentrations. The classical large time asymptotic scalings for this second order reaction with equal diffusivities in miscible fluids were found by Venzl [13] and Gálfi and Rácz [12]. Venzl found that the front position $X_f \sim T^{1/2}$ and further, Gálfi and Rácz determined that the reaction zone width $W_f \sim T^{1/6}$ and that the rate of production at the front $R_c \sim T^{-2/3}$. The scalings for the position of the front and width of the reaction zone were found to be in good agreement with experiments conducted in gels [14,15]. The short time and intermediate behaviors of this reaction for unequal diffusion coefficients was examined by Taitelbaum $et\ al.$ [16] who found that the reaction front could change direction under certain conditions.

Another common mechanism is $A + 2B \rightarrow C$, where now A is consumed at the rate kAB^2 and B is consumed at the rate $2kAB^2$. Cornell $et\ al.$ [8,9,17] considered, for miscible fluids with equal diffusion coefficients, the family of nonlinear reactions $nA + mB \rightarrow C$ with a rate of reaction $R_a = nkA^nB^m$ and $R_b = mkA^nB^m$ for species A and B, respectively. This altered the large time asymptotic scalings for the reaction zone width to $W_f \sim T^{1/2-\sigma}$ and the rate of production at the front to $R_c \sim T^{\sigma-1}$, where $\sigma = 1/(n+m+1)$. These results were then generalized by Koza [18] for arbitrary diffusion coefficients still for miscible fluids, with the large time scalings found to be unaffected. Sinder and Pelleg [19] obtained the solution for the product in miscible fluids for both a reversible and irreversible reaction.

In practice, complex reactions can also involve several intermediate steps such that the overall experimental kinetics yield reaction rates with fractional orders. This is the case for instance in complex reaction schemes in chain reactions, catalysis, or autocatalytic systems [20]. In this case the reaction rates $R_a = k_a A^n B^m$ and $R_b = k_b A^n B^m$ with n and m nonintegers and where k_a and k_b are not necessarily equal to nk and mk, respectively. This complex case has to our knowledge not been addressed theoretically yet, probably because of the lack of experimental studies of such complex kinetics in the case of initially separated species. From a theoretical point of view, analysis of such a general case is, however, interesting in the sense that it encompasses all other simpler cases at once.

The case for immiscible solvents has not been studied as extensively as the miscible fluids case. All the works that consider constant diffusion coefficients throughout the system analyze effectively miscible diluted solutions where the solvent of the solute species A and B is the same as, for instance, in two aqueous solutions of reactants A and B put in contact. If A and B are contained in miscible yet different solvents, then the diffusion coefficient of the solutes are spatially dependent when the two solvents start to mix. This situation is very difficult to analyze and will not be addressed here. Let us only mention a first step into such a direction which is the work by Polanowski and Koza [21] who recently examined the reaction $A + B \rightarrow 2C$ where the diffusion coefficients are taken as linear functions of the spatially dependent concentrations to extend the validity of the equations to more concentrated solutions. They found that the time scalings were affected by the diffusion coefficient of the product.

The presence of a physical interface in the problem has recently also attracted attention. In that regard, Chopard $et\ al.$ [11] theoretically examined the presence of a semipermeable wall upon the reaction $A + B \rightarrow C$ in which one species was unaffected by the wall whilst the other was not permitted to pass through the wall. Park $et\ al.$ [22] experimentally studied dynamics in a system with a semipermeable membrane and found that the large time scalings were unaffected by the membrane.

In this context, it is the goal of this paper to generalize previous analytical studies of asymptotic concentration profiles in reaction-diffusion systems by considering the cases with a general reaction rate A^nB^m in an immiscible two-layer system. This corresponds to a reactor in which a physical interface between two immiscible solvents is present and both reactive species A, B or the product C can cross the interface. We derive analytically large time asymptotic solutions for both the reactants and the product concentrations taking the partition coefficients as well as the diffusivity of the various chemical species in each liquid into consideration. The limit here deals with the class of moving boundary problems of the Stefan type (see Crank [23]). The theoretical scalings obtained are found to be unaltered by the fact that the fluids are immiscible. Some interesting asymptotic results obtained yields the following main conclusions: the reaction front in immiscible fluids can travel in the opposite direction to the one in miscible fluids, the total amount of product produced in time is independent of the rate of the reaction and the center of mass of the product can move in the opposite direction to the propagation of the front.

To explain these results, the paper is organized as follows. In Sec. II, the model and relevant parameters are introduced. The properties of the diffusive system in the absence of any reaction are underlined in Sec. III before the reaction-diffusion case is analyzed in detail in Sec. IV and V. The analytical asymptotic concentration profiles for immiscible systems are presented in Sec. IV. The properties of the front such as the front position, speed, and width as well as the amount of product produced in time are discussed in Sec. V before conclusions are drawn. In Appendix A the concentration equations within the reaction zone are derived. In Appendix B the inner and outer solutions are matched, yielding a single ODE. In Appendix C the position and width of the reaction front are obtained.

II. REACTION-DIFFUSION MODEL

Consider two immiscible solvents placed in contact along a planar interface. The left solvent contains a reactant A while the right one contains the reactant B. This study examines the family of chemical reactions whose reaction rate is proportional to $A^n B^m$ where n and m are positive constants. The mean field approximation is assumed and the rate of production is thus given by $R_j^{(i)} = k_j^{(i)} A^n B^m$, where $j = a, b, c$ so that $R_j^{(i)}$ depends on the chemical species considered and the superscript i is used to distinguish between the two liquids where $i = 1$ denotes the left liquid ($X < 0$) and $i = 2$ denotes the right liquid ($X > 0$)—note that the interface is located at $X = 0$ for all $T \geq 0$. The kinetic constants $k_a^{(i)}$, $k_b^{(i)}$, and $k_c^{(i)}$ are constants that may depend on the solvent. If the solvents are very different, the reaction mechanism can change leading to different kinetic equations and rate constants. However, here we assume that the reaction mechanism is the same in each solvent. For an elementary $nA + mB \rightarrow C$ reaction step, n and m are positive integers and the kinetic constants satisfy $k_a^{(i)} = nk_c^{(i)}$ and $k_b^{(i)} = mk_c^{(i)}$. However, for more complex reaction schemes, the detailed succession of elementary steps might be unknown while kinetic studies show that the global reaction rate is proportional to $A^n B^m$. In this case, n and m are no longer required to be integers and further, the constants $k_a^{(i)}$, $k_b^{(i)}$, and $k_c^{(i)}$ can be independent of n and m.

In the interest of generality, we seek therefore analytical solutions to the general system of one-dimensional reaction-diffusion equations given by

$$A_T = D_a^{(i)} A_{XX} - k_a^{(i)} A^n B^m, \tag{3a}$$

$$B_T = D_b^{(i)} B_{XX} - k_b^{(i)} A^n B^m, \tag{3b}$$

$$C_T = D_c^{(i)} C_{XX} + k_c^{(i)} A^n B^m. \tag{3c}$$

The subscripts X and T denote partial derivatives with respect to space and time. We note that this system is also valid in both two- and three-dimensional space when transverse instabilities of the front are absent.

The molecular diffusion coefficients $D_a^{(i)}$, $D_b^{(i)}$, and $D_c^{(i)}$ are constants that depend on the solvent. Thus for immiscible liquids each species will diffuse at a different rate in each of the solvents. In addition, the difference in solubility of the chemical species in both liquids is characterized by a partition coefficient p constant at equilibrium. Absorption and desorption rates are typically large so the interface shall be assumed to be sufficiently close to equilibrium and we are ignoring surfactants that can accumulate at the interface. Hence, we assume that the interface is in equilibrium with its surroundings so that we can introduce the partition coefficients p_a, p_b, and p_c defined as

$$p_a = \frac{A^{(1)}}{A^{(2)}}, \quad p_b = \frac{B^{(1)}}{B^{(2)}}, \quad p_c = \frac{C^{(1)}}{C^{(2)}}, \tag{3d}$$

where the concentration in each liquid is evaluated at the interface $X = 0$. At the interface we also require a flux balance for each species, yielding

$$\frac{D_a^{(1)}}{D_a^{(2)}} A_X^{(1)} = A_X^{(2)}, \quad \frac{D_b^{(1)}}{D_b^{(2)}} B_X^{(1)} = B_X^{(2)}, \quad \frac{D_c^{(1)}}{D_c^{(2)}} C_X^{(1)} = C_X^{(2)}. \tag{3e}$$

The domain is considered sufficiently large to be modeled as infinite. Thus, at infinity we apply no flux boundary conditions.

$$A_X^{(1)}, B_X^{(1)}, C_X^{(1)} \rightarrow 0 \quad \text{as } X \rightarrow -\infty, \tag{3f}$$

$$A_X^{(2)}, B_X^{(2)}, C_X^{(2)} \rightarrow 0 \quad \text{as } X \rightarrow \infty. \tag{3g}$$

Finally, we have the initial conditions

$$A^{(1)} = A_0, \quad B^{(2)} = B_0, \quad B^{(1)} = A^{(2)} = C^{(1)} = C^{(2)} = 0, \tag{3h}$$

where A_0 and B_0 are the initial concentrations of reactants A and B in the left and right liquids, respectively. This condition means that all of the species are initially homogeneous in each semi-infinite region with one only containing A whilst the other only contains B.

To nondimensionalize this set of equations, characteristic length and time scales are constructed using the kinetic constant and diffusion coefficient in liquid 2, i.e., we take

$$l_0 = \left(\frac{D_a^{(2)}}{k_a^{(2)} A_0^{n+m-1}} \right)^{1/2} \quad \text{and} \quad t_0 = \frac{1}{k_a^{(2)} A_0^{n+m-1}}. \tag{4}$$

We introduce the following dimensionless variables $x = X/l_0$, $t = T/t_0$, $a = A/A_0$, $b = B/A_0$, and $c = C/A_0$. The dimensionless parameters are typically the ratio ϕ of initial reactant concentrations

$$\phi = \frac{B_0}{A_0}, \tag{5a}$$

the ratios κ_a, κ_b, κ_c, ψ, and ξ of kinetic constants

$$\kappa_a = \frac{k_a^{(1)}}{k_a^{(2)}}, \quad \kappa_b = \frac{k_b^{(1)}}{k_a^{(2)}}, \quad \kappa_c = \frac{k_c^{(1)}}{k_a^{(2)}}, \quad \psi = \frac{k_b^{(2)}}{k_a^{(2)}}, \quad \xi = \frac{k_c^{(2)}}{k_a^{(2)}}, \tag{5b}$$

and the ratios of diffusion coefficients q, r, s, $\hat{r}$, and $\hat{s}$ defined, respectively, as

$$q = \sqrt{\frac{D_a^{(2)}}{D_a^{(1)}}}, \quad r = \sqrt{\frac{D_a^{(2)}}{D_b^{(2)}}}, \quad s = \sqrt{\frac{D_a^{(2)}}{D_c^{(2)}}},$$

$$\hat{r} = \sqrt{\frac{D_a^{(2)}}{D_b^{(1)}}}, \quad \hat{s} = \sqrt{\frac{D_a^{(2)}}{D_c^{(1)}}}. \tag{5c}$$

We will assume here that the chemical front invades layer 2 (the symmetric situation where the front invades liquid 1 being trivial to obtain). Now, the physical measurable dimensional quantities such as the rate of production $R_c^{(2)}$, position X_f, and width W_f of the front can be transformed into their equivalent dimensionless quantities as $R = R_c^{(2)} t_0 / A_0$, $x_f = X_f / l_0$, and $w_f = W_f / l_0$, where

$$R = \xi a^n b^m, \quad x_f = \frac{\int_{-\infty}^{\infty} Rx\,dx}{\int_{-\infty}^{\infty} R\,dx}, \quad w_f^2 = \frac{\int_{-\infty}^{\infty} R(x - x_f)^2 dx}{\int_{-\infty}^{\infty} R\,dx}. \tag{6}$$

The dimensionless equations in liquid 1 at the left are then

$$a_t^{(1)} = \frac{a_{xx}^{(1)}}{q^2} - \kappa_a a^{(1)^n} b^{(1)^m}, \tag{7a}$$

$$b_t^{(1)} = \frac{b_{xx}^{(1)}}{\hat{r}^2} - \kappa_b a^{(1)^n} b^{(1)^m}, \tag{7b}$$

$$c_t^{(1)} = \frac{c_{xx}^{(1)}}{\hat{s}^2} + \kappa_c a^{(1)^n} b^{(1)^m}, \tag{7c}$$

while we have in liquid 2 located to the right,

$$a_t^{(2)} = a_{xx}^{(2)} - a^{(2)^n} b^{(2)^m}, \tag{7d}$$

$$b_t^{(2)} = \frac{b_{xx}^{(2)}}{r^2} - \psi a^{(2)^n} b^{(2)^m}, \tag{7e}$$

$$c_t^{(2)} = \frac{c_{xx}^{(2)}}{s^2} + \xi a^{(2)^n} b^{(2)^m}. \tag{7f}$$

On $x=0$, the boundary conditions (3d) and (3e) become

$$a^{(1)} = p_a a^{(2)}, \quad b^{(1)} = p_b b^{(2)}, \quad c^{(1)} = p_c c^{(2)}, \tag{7g}$$

$$a_x^{(1)} = q^2 a_x^{(2)}, \quad r^2 b_x^{(1)} = \hat{r}^2 b_x^{(2)}, \quad s^2 c_x^{(1)} = \hat{s}^2 c_x^{(2)}. \tag{7h}$$

The far field boundary conditions (3f) and (3g) are now

$$a_x^{(1)}, b_x^{(1)}, c_x^{(1)} \rightarrow 0 \quad \text{as } x \rightarrow -\infty, \tag{7i}$$

$$a_x^{(2)}, b_x^{(2)}, c_x^{(2)} \rightarrow 0 \quad \text{as } x \rightarrow \infty, \tag{7j}$$

while at $t=0$, the initial condition (3h) reads

$$a^{(1)} = 1, \quad b^{(2)} = \phi, \quad b^{(1)} = a^{(2)} = c^{(1)} = c^{(2)} = 0. \tag{7k}$$

Notice that, in an infinite domain, the no flux far field boundary conditions are effectively equivalent to having the concentrations specified at their initial values.

III. NONREACTIVE SYSTEM

For comparative purposes, it is useful to first recall the properties of the concentration profiles in the absence of reactions. Then, the equations are linear, decoupled, and with constant coefficients in each half space. When there is no reaction, there is no product so that $c^{(1)} = c^{(2)} = 0$. The remaining four diffusion equations are

$$a_t^{(1)} = \frac{a_{xx}^{(1)}}{q^2}, \quad b_t^{(1)} = \frac{b_{xx}^{(1)}}{\hat{r}^2}, \tag{8a}$$

$$a_t^{(2)} = a_{xx}^{(2)}, \quad b_t^{(2)} = \frac{b_{xx}^{(2)}}{r^2}. \tag{8b}$$

We introduce the similarity variable

$$\eta = \frac{x}{2\sqrt{t}}, \tag{9}$$

which allows the far field boundary conditions (7i) and (7j) to transform into the initial conditions (7k). The bulk equations in Eqs. (8) and boundary conditions (7g) and (7j) are satisfied by the analytical solutions [23,24]

$$a^{(1)} = 1 - q\frac{\text{erfc}(-q\eta)}{p_a + q}, \quad a^{(2)} = \frac{\text{erfc}(\eta)}{p_a + q}, \tag{10a}$$

$$b^{(1)} = \phi\hat{r}p_b\frac{\text{erfc}(-\hat{r}\eta)}{\hat{r} + rp_b}, \quad b^{(2)} = \phi\left[1 - rp_b\frac{\text{erfc}(r\eta)}{\hat{r} + rp_b}\right]. \tag{10b}$$

The above solution (10) for two immiscible fluids can be reduced to the solution for two miscible fluids by setting the partition coefficients $p_a = p_b = 1$ and equating the diffusion coefficients $D_a^{(1)} = D_a^{(2)} = D_a$, $D_b^{(1)} = D_b^{(2)} = D_b$ so that $q=1$ and $\hat{r} = r$. One obtains then for miscible nonreactive fluids,

$$a^{(1)} \equiv a^{(2)} = \frac{\text{erfc}(\eta)}{2}, \quad b^{(1)} \equiv b^{(2)} = \phi\frac{\text{erfc}(-\tilde{r}\eta)}{2}, \tag{11}$$

where $\tilde{r}$ is here simply equal to $\sqrt{D_a/D_b}$. Solutions (10) and (11) are valid for all time and give the concentration profiles of species A and B after contact for, respectively, immiscible and miscible solvents each initially containing a different species. For the miscible fluids, one recovers the classical solution (11) depending only on the ratio of initial concentrations ϕ and on $\tilde{r} = \sqrt{D_a/D_b}$. On the contrary, for immiscible fluids, the solutions in Eqs. (10) depend not only on ϕ, but also on the ratios of the diffusion coefficients in each phase q, r, $\hat{r}$ and on the partition coefficients p_a and p_b.

In Fig. 1 typical concentration profiles of a against η are plotted to illustrate the difference between the immiscible and miscible nonreactive cases. For the miscible case, solution (11) is symmetric with regard to $\eta=0$ which is not the case in the immiscible situation. As an example, Fig. 1 shows the profiles for the immiscible case when $q = \frac{1}{2}$ so that species A diffuses four times faster in liquid 1 than in liquid 2. When $p_a = 1$ so that A has the same solubility in both liquids [Fig. 1(b)], a larger diffusivity of species A in liquid 1 leads to higher concentrations in liquid 2. Depending on whether the solubility of A in liquid 1 is larger [$p_a > 1$, Fig. 1(a)] or smaller [$p_a < 1$, Fig. 1(c)] than in liquid 2, the concentration of A in the left liquid 1 will be larger or smaller, respectively, than in the miscible case. Furthermore, in that latter case, the concentration of A in liquid 2 at the interface can even become greater than the initial concentration in liquid 1 as can be seen in Fig. 1(c). From Eqs. (10) the condition for this to occur is that $p_a + q < 1$. Similarly, for species B to have a greater concentration in liquid 1 at the interface than the initial concentration in liquid 2 requires that $\frac{1}{p_b} + \frac{r}{\hat{r}} < 1$ in the case of immiscible systems.
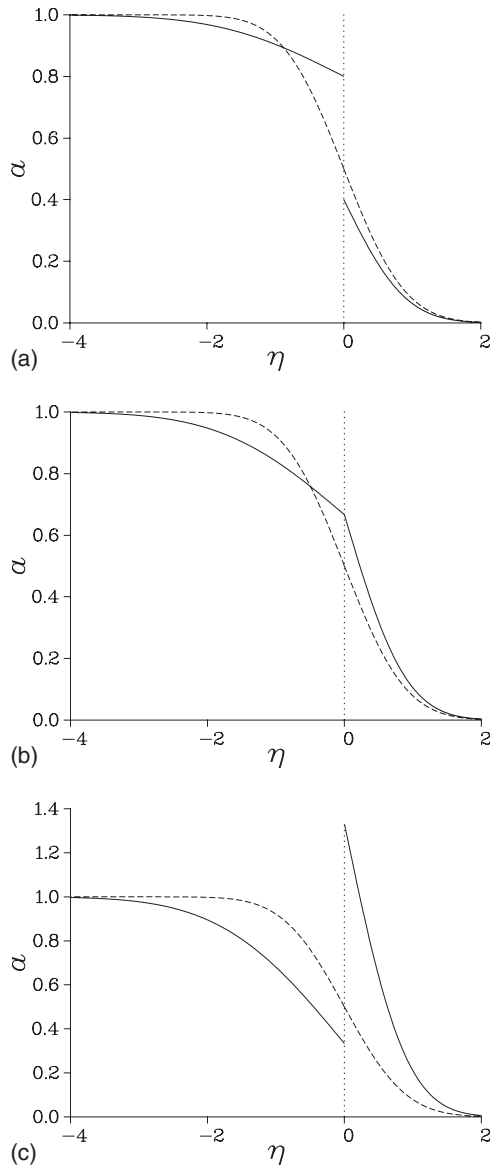
FIG. 1. Diffusive concentration profiles for species A against $\eta = x/\sqrt{4t}$ in the absence of any reaction for, respectively, the miscible (dashed) and immiscible (full) cases. The miscible case corresponds to $q = p_a = 1$, whilst the immiscible case is represented with a ratio of diffusion coefficient $q = \frac{1}{2}$ and various values of the partition coefficient: (a) $p_a = 2$, (b) $p_a = 1$, and (c) $p_a = \frac{1}{4}$. The dotted line represents the interface at $\eta = 0$.

IV. REACTIVE SYSTEMS: LARGE TIME ASYMPTOTICS

In the presence of a chemical reaction, a narrow reaction zone is formed at the location where the reaction-diffusion terms are balanced. Outside the reaction zone one of the reactants will be virtually exhausted so that no reaction takes place. We call this the "outer region." The outer region is a purely diffusive region where lengths scale with $\sqrt{t}$. The reaction zone width w_f is anticipated to increase at a slower rate than $\sqrt{t}$, so that for large times the reaction front width is negligible compared to the diffusive length scale. Hence, the reaction zone will be treated like a single point where both a and b vanish. We define $x_f(t)$ as the point where the outer
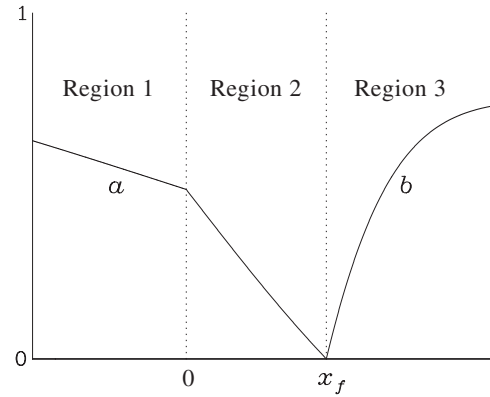

FIG. 2. A sketch of regions 1, 2, and 3. Full lines denote the concentrations a and b. Dotted lines denote $x = 0$ (location of the interface between the two immiscible fluids) and $x = x_f$ (location of the reaction front).

solution $a(x_f(t), t) = 0$. Seeking a similarity solution leads to the equation

$$x_f(t) = 2\alpha\sqrt{t}, \qquad (12)$$

where α is an unknown constant that determines the reaction front wave speed [see Eq. (5) in Gálfi and Rácz [12]]. The front can, in principle, invade either of the phases, depending on the parameters. For concreteness we will assume as mentioned above that the front moves to the right into the $x > 0$ layer, i.e., $\alpha > 0$. The condition on the parameters consistent with this assumption will be derived.

The presence of a moving front requires that the right domain ($x > 0$) is now itself divided into two regions: Region 2 is redefined as the zone where $0 < x < x_f(t)$ and we introduce region 3 defined as the remaining zone where $x_f(t) < x$. This layout is sketched in Fig. 2. No reaction takes place in the outer region where one of the species has been exhausted, i.e., $b^{(1)} = b^{(2)} = a^{(3)} = 0$, where the subscript $i = 1, 2, 3$ denotes the region where the concentration is evaluated. The six remaining transport equations in the outer region where the reaction is negligible are

$$a_t^{(1)} = \frac{a_{xx}^{(1)}}{q^2}, \quad c_t^{(1)} = \frac{c_{xx}^{(1)}}{\hat{s}^2}, \qquad (13a)$$

$$a_t^{(2)} = a_{xx}^{(2)}, \quad c_t^{(2)} = \frac{c_{xx}^{(2)}}{s^2}, \qquad (13b)$$

$$b_t^{(3)} = \frac{b_{xx}^{(3)}}{r^2}, \quad c_t^{(3)} = \frac{c_{xx}^{(3)}}{s^2}. \qquad (13c)$$

Using the similarity variable η defined in Eq. (9), the analytical solutions are obtained and twelve constants are introduced. Four constants are determined from the interfacial conditions at $\eta = 0$.

$$a^{(1)} = p_a a^{(2)}, \quad c^{(1)} = p_c c^{(2)}, \quad a_\eta^{(1)} = q^2 a_\eta^{(2)}, \quad s^2 c_\eta^{(1)} = \hat{s}^2 c_\eta^{(2)},$$

where the subscript η indicates derivatives with respect to η. Four more constants are determined from the far field conditions.

$$a^{(1)} \rightarrow 1, \quad c^{(1)} \rightarrow 0 \quad \text{as } \eta \rightarrow -\infty,$$

$$b^{(3)} \rightarrow \phi, \quad c^{(3)} \rightarrow 0 \quad \text{as } \eta \rightarrow \infty.$$

These conditions are equivalent to the initial conditions. Three further constants are determined by setting $a^{(2)} = b^{(3)} = 0$ and $c^{(2)} = c^{(3)}$ on $x = x_f(t)$. One remains thus with one additional constant h and, for immiscible reactive two-layer systems, we obtain the outer solution profiles

$$a^{(1)} = 1 - q \frac{\text{erfc}(-q\eta)}{q + p_a \text{erf}(\alpha)}, \quad c^{(1)} = h \frac{\hat{s} p_c \text{erfc}(-\hat{s}\eta)}{\hat{s} + sp_c \text{erf}(s\alpha)},$$
(14a)

$$a^{(2)} = \frac{\text{erfc}(\eta) - \text{erfc}(\alpha)}{q + p_a \text{erf}(\alpha)}, \quad c^{(2)} = h \frac{\hat{s} + sp_c \text{erf}(s\eta)}{\hat{s} + sp_c \text{erf}(s\alpha)},$$
(14b)

$$b^{(3)} = \phi - \phi \frac{\text{erfc}(r\eta)}{\text{erfc}(r\alpha)}, \quad c^{(3)} = h \frac{\text{erfc}(s\eta)}{\text{erfc}(s\alpha)}.$$
(14c)

In the special case when the product c is insoluble in liquid 1 like in the experiments by Eckert *et al.* [1,2,4], the partition coefficient $p_c = 0$ and the solution for the product becomes simply

$$c^{(1)} = 0, \quad c^{(2)} = h, \quad c^{(3)} = h \frac{\text{erfc}(s\eta)}{\text{erfc}(s\alpha)}.$$

Solution (14) for two immiscible fluids can be reduced to a solution for the case of two miscible fluids by setting $p_a = p_c = q = 1$ and $s = \hat{s}$ to obtain

$$a^{(1)} \equiv a^{(2)} = 1 - \frac{\text{erfc}(-\eta)}{\text{erfc}(-\alpha)}, \quad b^{(3)} = \phi - \phi \frac{\text{erfc}(r\eta)}{\text{erfc}(r\alpha)},$$
(15a)

$$c^{(1)} \equiv c^{(2)} = h \frac{\text{erfc}(-s\eta)}{\text{erfc}(-s\alpha)}, \quad c^{(3)} = h \frac{\text{erfc}(s\eta)}{\text{erfc}(s\alpha)}.$$
(15b)

The constants α and h are obtained by balancing the reaction rates with the fluxes at the reaction front. The flux of species A into the reaction front divided by its rate of consumption equals the flux of species B into the reaction front divided by its rate of consumption which also equals the total flux of species C emerging from the reaction front divided by its rate of production. Thus using dimensional quantities we have

$$-\frac{D_a^{(2)}}{k_a^{(2)}} a_x^{(2)} = \frac{D_b^{(2)}}{k_b^{(2)}} b_x^{(3)} = \frac{D_c^{(2)}}{k_c^{(2)}} (c_x^{(2)} - c_x^{(3)}).$$
(16)

Hence we obtain

$$e^{\alpha^2(r^2-1)} \text{erfc}(r\alpha) = \frac{\phi}{\psi r} [q + p_a \text{erf}(\alpha)],$$
(17)

and

$$h = \frac{\xi s e^{\alpha^2(s^2-1)} \text{erfc}(s\alpha)[\hat{s} + sp_c \text{erf}(s\alpha)]}{[q + p_a \text{erf}(\alpha)][\hat{s} + sp_c]}.$$
(18)

Equivalent conditions are rigorously obtained by constructing an inner solution inside the reaction zone (see Appendix A) and matching this solution to the outer solution (see Appendix B). The resulting inner solutions are given by

$$a_I = \frac{U}{\lambda t^\sigma} G, \quad b_I = \frac{U\psi r^2}{\lambda t^\sigma}(G + z),$$
(19a)

$$c_I = h - \frac{U\xi s^2}{\lambda t^\sigma} \left(G + z \frac{\hat{s} + sp_c \text{erf}(s\alpha)}{\hat{s} + sp_c} \right),$$
(19b)

where $G(z)$ is the solution to system (B5a) and (B5b), $z = \frac{1}{2}\lambda(x - x_f)t^{\sigma - (1/2)}$, $\lambda = U(4\psi^m r^{2m}/U^2)^\sigma$, $\sigma^{-1} = n + m + 1$, and $U^{-1} = \frac{1}{2}\sqrt{\pi}[q + p_a \text{erf}(\alpha)]e^{\alpha^2}$. Thus the concentrations inside the reaction zone scale with $t^{-\sigma}$ and the width of the reaction zone scales with $t^{(1/2)-\sigma}$. As $\sigma > 0$, the reaction front width is smaller than the diffusive length scale $\sqrt{t}$, which justifies the assumption we made that the reaction zone can be modeled by a point. The validity of this solution was checked by comparing it with numerical solutions to system (7a)–(7k). Excellent agreement was found between the large time evolution of the full system of equations (7a)–(7k) and the analytical asymptotic solutions (14) and (19).

To compare to the miscible case we can put the partition coefficients equal to 1 and the diffusion coefficients of each species equal in liquid 1 and 2, i.e. we take $p_a = p_b = p_c = q = 1$, and $s = \hat{s}$. In this case Eq. (17) is equivalent to Eq. (24) by Koza [18] when $\psi = \frac{m}{n}$. If in addition $\psi = \xi = 1$, then Eq. (18) is the dimensionless version of Eq. (14) in Sinder and Pelleg [19] for the $A + B \rightarrow C$ reaction.

The constant α which gives the evolution of the front position x_f in time [see Eq. (12)] is the solution to the transcendental equation (17). Notice that the left-hand side of Eq. (17) is a monotonic decreasing function of α whilst the right-hand side is a monotonic increasing function of α, hence, there is at most one solution for α. In the special case when A and B diffuse at the same rates, i.e., when $r = 1$, then Eq. (17) can be rearranged to yield

$$\text{erf}(\alpha) = \frac{\psi - \phi q}{\psi + \phi p_a}.$$
(20)

A special case of this equation can be obtained from Eq. (6) in Cornell *et al.* [9] for the case of miscible fluids for a single stage reaction with $\psi = m/n$, $q = 1$, and $p_a = 1$.

To illustrate the contraction of the reaction zone in time, a, b, and c are plotted against η at $t = 10^3$ and $t = 10^6$ in Fig. 3 for a single set of parameter values with $w^* = w_f/(2\sqrt{t}) \sim t^{-1/3}$. In Fig. 3, unity partition coefficients have been chosen to yield continuous concentrations at the interface in order to highlight the change in the concentration gradients at the interface due to the change in the diffusive rates between each liquid.
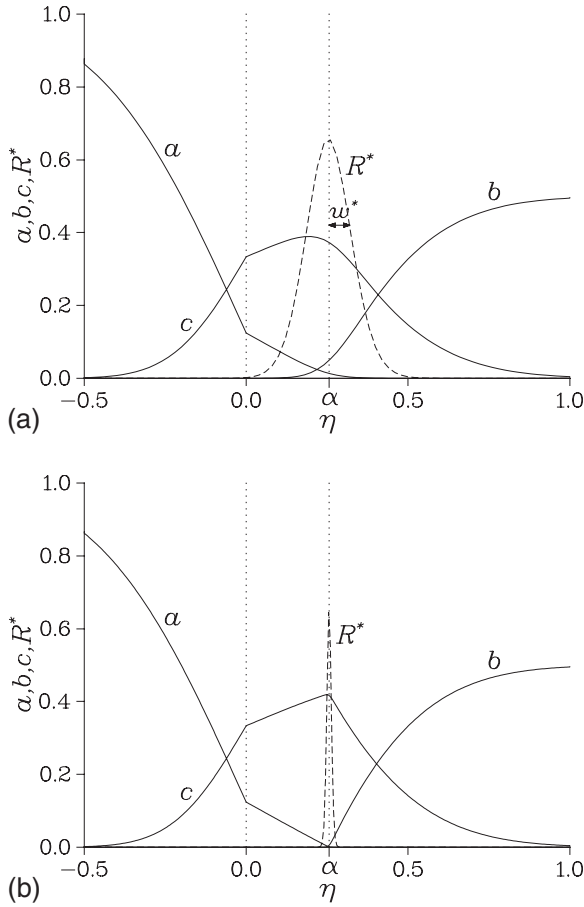
FIG. 3. Concentrations as a function of η (a) at $t=10^3$ and (b) at $t=10^6$ for $q=r=s=2$, $\hat{s}=\hat{r}=4$, $\phi=\frac{1}{2}$, $n=m=\kappa_a=\kappa_b=\kappa_c=p_a=p_b=p_c$ $=\psi=\xi=1$. To better visualize the tiny reaction zone, we plot here a rescaled rate of production $R^*=10abt^{2/3}$ and $w^*=w_f/(2\sqrt{t})$. The dotted lines denote the interface at $\eta=0$ and the asymptotic first moment of the reaction zone at $\eta=\alpha$.

V. PROPERTIES OF THE REACTION FRONT

Using the asymptotic outer solutions (14) derived, let us analyze the ensuing properties of the reaction front. In Appendix C, the first moment of the production rate is shown to indeed be given by Eq. (12), namely, $x_f=2\alpha\sqrt{t}$, and further, the reaction front width is shown to be given by

$$w_f=\{\sqrt{\pi t}[q+p_a \text{ erf}(\alpha)]e^{\alpha^2}\}^{1-2\sigma}\frac{\sqrt{I}}{(\psi r^2)^{m\sigma}}, \qquad (21)$$

where I is a constant, defined in Appendix C, that only depends on n and m. The presence of the interface can have a dramatic effect on the speed of the reaction front, however, the effect on the width of the reaction front is much weaker. Figures 4 and 5 illustrate the effects of the presence of an interface on the temporal dependence of the asymptotic front position x_f predicted from Eq. (12) and of the asymptotic front width w_f predicted from Eq. (21) for various parameter cases. They show that increasing p_a or q or decreasing r cause the reaction front to move slower (see Figs. 4), but the width of the reaction front gets larger (see Fig. 5).
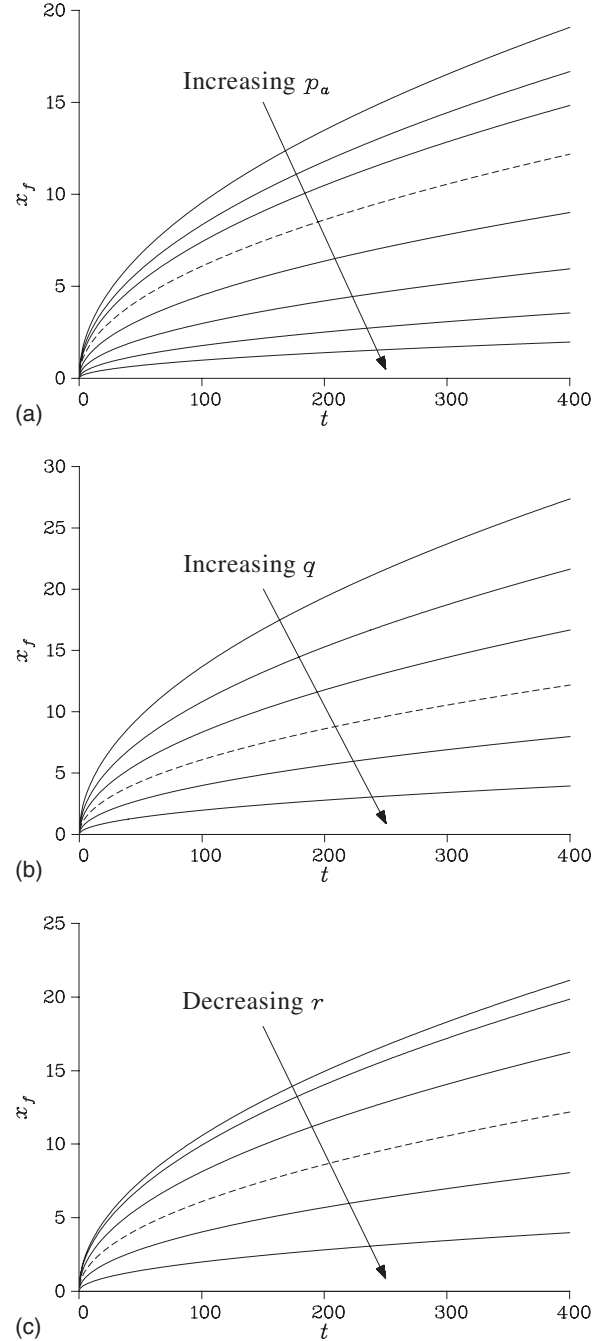

FIG. 4. Temporal dependence of the position x_f of the reaction front for various values of the partition coefficient p_a (a), and of the ratio of the diffusion coefficients q (b) and r (c). In (a) p_a $=0,\frac{1}{4},\frac{1}{2},1,2,4,8,16$, in (b) $q=0,\frac{1}{3},\frac{2}{3},1,\frac{4}{3},\frac{5}{3},2$, and in (c) r $=\frac{1}{2},\frac{3}{5},\frac{3}{4},1,\frac{3}{2},3,6$. Except where stated the parameter values are $\phi=\frac{1}{2}$ and $q=r=s=\hat{s}=\hat{r}=n=m=\kappa_a=\kappa_b=\kappa_c=p_a=p_b=p_c=\psi=\xi=1$. The dashed lines correspond to the miscible fluids case when (a) $p_a=1$, (b) $q=1$, and (c) $r=\hat{r}$. The lines corresponding to $q=2$ in (b) and $r=\frac{1}{2}$ in (c) coincide with $x_f=0$.

A. Position of the front

The position of the front x_f depends linearly on $\alpha(\frac{\phi}{\psi},r,q,p_a)$, which is the solution to Eq. (17). [Although α is independent of n and m for complicated kinetics with frac-
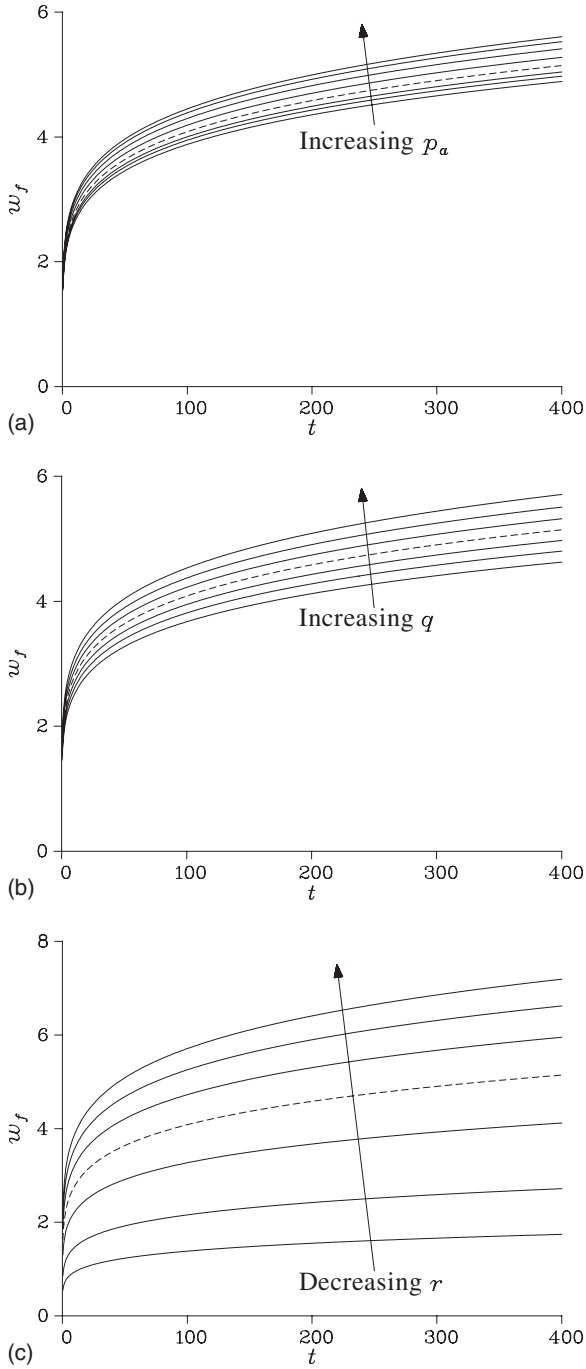
FIG. 5. Temporal dependence of the width of the front w_f for various values of the partition coefficient p_a (a), and of the ratio of the diffusion coefficients q (b) and r (c). The parameter values are the same as those in Fig. 4.

tional orders, in the case of an elementary reaction step $\psi \equiv m/n$ so that n and m can affect α]. By expanding Eq. (17) in small α we obtain the approximation

$$\alpha \simeq \frac{\sqrt{\pi}}{2} \frac{\psi r - \phi q}{\psi r^2 + \phi p_a} \quad \text{for } 0 \leq \frac{\psi r}{\phi q} - 1 \ll 1. \quad (22)$$

The condition for the front to move to the right, i.e., for a non-negative solution for α to exist, requires $\phi q \leq \psi r$. In

conditions for which this equality is satisfied and the front thus invades liquid 2, we find that increasing ϕ (i.e., increasing B_0 over A_0), q (i.e., increasing the diffusivity of A in liquid 2 compared to liquid 1), or p_a (i.e., increasing the solubility of A in liquid 1 compared to liquid 2) reduce α. On the contrary, increasing ψ (i.e., increasing the rate of consumption of B over that of A) or r (i.e., increasing the diffusivity of A compared to B in liquid 2) leads to an increase in α.

It should be noted that the solubility of the species has no effect on the direction of the front, since p_a cannot alter the sign of α; however, as effectively stated in the previous sentence, the solubility does affect the magnitude of the front speed. In particular, in the large p_a limit, α tends to zero, which physically corresponds to reducing the solubility of species A in liquid 2 making it more difficult for species A and hence the reaction front, to invade liquid 2.

Recalling the parameter definitions given in Eq. (5a)–(5c), for $\alpha \geq 0$, i.e., $\phi q \leq \psi r$, this amounts to satisfying the condition

$$\frac{B_0}{A_0} \frac{k_a^{(2)}}{k_b^{(2)}} \leq \sqrt{\frac{D_a^{(1)}}{D_b^{(2)}}}, \quad (23)$$

with a stationary front occurring at equality. A special case of this was studied numerically [25] and confirmed analytically [see Eq. (26) of Ref. [18]] for the reaction $A + B \rightarrow C$ in miscible fluids for which $k_a^{(2)} = k_b^{(2)}$. For equimolar initial concentrations ($A_0 = B_0$) and when $k_a^{(2)} = k_b^{(2)}$, the front remains stationary ($\alpha = 0$) only if $D_a^{(1)} = D_b^{(2)}$. This is a constraining condition as different chemical species rarely have exactly the same diffusion coefficient. As a consequence, in the vast majority of situations, the equality of Eq. (23) is not satisfied, the front will move, and $\alpha \neq 0$.

A consequence of Eq. (23) is that, for immiscible systems, the direction of the front is independent of $D_a^{(2)}$. Rearranging Eq. (23), the condition for $\alpha > 0$ in two immiscible liquids is

$$D_b^{(2)} \left(\frac{B_0 k_a^{(2)}}{A_0 k_b^{(2)}} \right)^2 \leq D_a^{(1)}, \quad (24a)$$

whilst if the same reaction is carried out in two miscible liquids, with both liquids having the same properties as liquid 2, then the condition for $\alpha < 0$ is

$$D_a^{(2)} \leq D_b^{(2)} \left(\frac{B_0 k_a^{(2)}}{A_0 k_b^{(2)}} \right)^2. \quad (24b)$$

Hence, as long as $D_a^{(1)} \neq D_a^{(2)}$, then there exists a range of parameter values in which a reaction front formed by two immiscible fluids can travel in the opposite direction to the reaction front formed by two miscible fluids.

B. Speed of the front

The relationship between each of the physical variables and the speed of the reaction front can easily be identified from the dependence of α upon the dimensionless variables and so a summary of the effects of the various physical parameters upon the front position and hence its speed are

TABLE I. Parameter effects upon the position (x_f and dimensional X_f) and width (w_f and dimensional W_f) of a front invading liquid 2 when the remaining parameters are fixed. The $+$ sign corresponds to the case when increasing a parameter causes an increase in a physical property, the $-$ sign corresponds to the reverse of this, and the $\pm$ sign corresponds to a parameter that can both increase or decrease. The special case where $n=m=1$ is shown in the two last columns.

			$n=m=1$	
Parameter	x_f	X_f	w_f	W_f
$D_a^{(2)}$, diffusivity of A in liquid 2	$\pm$	$+$	$\pm$	$+$
$D_a^{(1)}$, diffusivity of A in liquid 1	$+$	$+$	$-$	$-$
$D_b^{(2)}$, diffusivity of B in liquid 2	$-$	$-$	$+$	$+$
A_0, initial concentration of A	$+$	$+$	$+$	$-$
B_0, initial concentration of B	$-$	$-$	$-$	$-$
$k_a^{(2)}$, rate of consumption of A in liquid 2	$-$	$-$	$+$	$-$
$k_b^{(2)}$, rate of consumption of B in liquid 2	$+$	$+$	$-$	$-$
p_a, solubility of A in liquid 1/liquid 2	$-$	$-$	$+$	$+$

given in Table I. It is seen that all effects favoring the invasion of liquid 2 by the reactant A contained initially only in liquid 1 will lead to a front traveling faster to the right, when $\alpha > 0$. For both miscible and immiscible systems with $\alpha > 0$ increasing the initial concentration of A, increasing the diffusivity of A, or reducing the rate of consumption of A lead to increases in the front speed whilst the opposite effect occurs when the corresponding changes are made to the parameters associated with B. For immiscible systems, increasing the solubility of A into layer 2 favors also the invasion of this layer by the chemical front.

The effective influence of $D_a^{(2)}$ is more complicated to isolate since it affects both q and r: increasing $D_a^{(2)}$ increases both of these parameters, however, increasing q causes α to decrease whilst increasing r causes α to increase. Thus α has a nontrivial dependence on $D_a^{(2)}$, hence the $\pm$ sign in Table I for the influence of $D_a^{(2)}$ on the dimensionless quantities x_f and w_f. However, in dimensional quantities the position of the front is given by

$$X_f = 2\alpha\sqrt{D_a^{(2)}T}, \qquad (25)$$

and we find that increasing $D_a^{(2)}$ causes $\alpha\sqrt{D_a^{(2)}}$ to increase, and hence the front speed increases.

C. Width of the front

Interestingly, varying the parameters does not always have the same influence on the front width and front speed (see Table I). Indeed, the position of the reaction front always scales with $\sqrt{t}$, however, the width of the reaction front scales with $t^{(1/2)-\sigma}$, so that when $\sigma < \frac{1}{2}$ the width tends to infinity in the course of time while when $\sigma > \frac{1}{2}$ the width tends on the contrary to zero. As a consequence and as $\sigma = 1/(n+m+1)$, larger values of n and m yield wider reaction zones. Physically, for elementary reactions, $n+m > 1$ so that the case $\sigma < \frac{1}{2}$ may be irrelevant in that case. When $n+m > 1$, it can be shown that increasing p_a or q causes w_f to

increase, whilst increasing ϕ causes w_f to decrease; the reverse holds when $n+m < 1$. Returning to dimensional quantities the width of the front is given by

$$W_f = \frac{(D_a^{(2)})^{(1/2)-m\sigma}(D_b^{(2)})^{m\sigma}}{(k_a^{(2)})^{\sigma-m\sigma}(k_b^{(2)})^{m\sigma}}$$
$$\times \left[\frac{\sqrt{\pi T}}{A_0}\left(\sqrt{\frac{D_a^{(2)}}{D_a^{(1)}}} + p_a\,\mathrm{erf}(\alpha) \right)e^{\alpha^2} \right]^{1-2\sigma}\sqrt{I}.$$

Notice that in dimensional quantities Eq. (17) is

$$\sqrt{\frac{D_a^{(2)}}{D_a^{(1)}}} + p_a\,\mathrm{erf}(\alpha) = \frac{k_b^{(2)}A_0\sqrt{D_a^{(2)}}}{k_a^{(2)}B_0\sqrt{D_b^{(2)}}}$$
$$\times\mathrm{erfc}\left(\alpha\sqrt{\frac{D_a^{(2)}}{D_b^{(2)}}} \right)\frac{e^{\alpha^2(D_a^{(2)}/D_b^{(2)})}}{e^{\alpha^2}}.$$

In the most common case where $n=m=1$ and using the previous relation we obtain

$$W_f = \left[\frac{D_b^{(2)}\sqrt{\pi D_a^{(2)}T}}{A_0 k_b^{(2)}}\left(\sqrt{\frac{D_a^{(2)}}{D_a^{(1)}}} + p_a\,\mathrm{erf}(\alpha) \right)e^{\alpha^2} \right]^{1/3}\sqrt{I} \quad (26a)$$

$$= \left[\frac{D_a^{(2)}\sqrt{\pi D_b^{(2)}T}}{B_0 k_a^{(2)}}\,\mathrm{erfc}\left(\alpha\sqrt{\frac{D_a^{(2)}}{D_b^{(2)}}} \right)e^{\alpha^2(D_a^{(2)}/D_b^{(2)})} \right]^{1/3}\sqrt{I} \quad (26b)$$

$$= (D_a^{(2)}D_b^{(2)})^{1/4}\left[\mathrm{erfc}\left(\alpha\sqrt{\frac{D_a^{(2)}}{D_b^{(2)}}} \right) \right]^{1/6}\sqrt{I}$$
$$\times \left[\frac{\pi T e^{\alpha^2[(D_a^{(2)}+D_b^{(2)})/D_b^{(2)}]}}{A_0 B_0 k_b^{(2)}k_a^{(2)}} \right]^{1/6}\left(\sqrt{\frac{D_a^{(2)}}{D_a^{(1)}}} + p_a\,\mathrm{erf}(\alpha) \right)^{1/6}. \quad (26c)$$

The first expression for W_f, Eq. (26a), reveals that increasing $k_a^{(2)}$ or B_0, which both decrease α, cause W_f to decrease since $\mathrm{erf}(x)e^{x^2}$ is an increasing function of x. The second expression, Eq. (26b), reveals that increasing $k_b^{(2)}$, A_0, or $D_a^{(1)}$, which
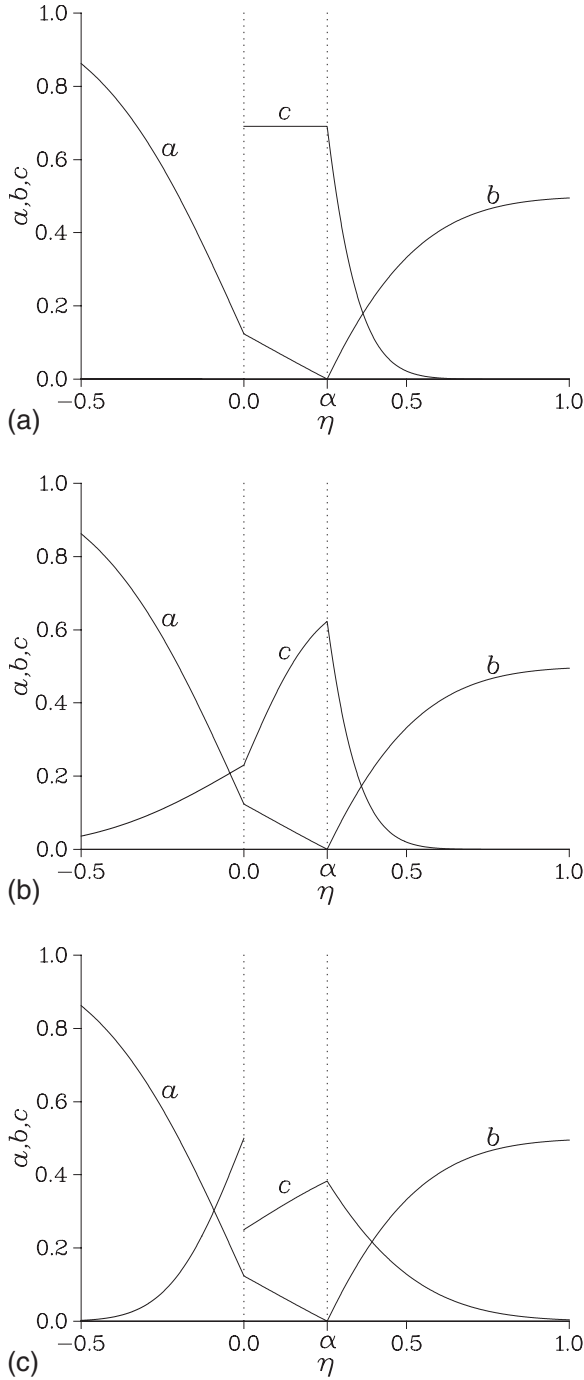
FIG. 6. Analytical outer solutions for (a) $p_c=0$, $\hat{s}=2$, $s=4$; (b) $p_c=1$, $\hat{s}=2$, $s=4$; and (c) $p_c=2$, $\hat{s}=4$, $s=2$. The dotted lines denote the interface at $\eta=0$ and the reaction front at $\eta=\alpha$. The remaining parameter values are $q=r=2$, $\phi=\frac{1}{2}$, and $p_a=\psi=\xi=1$. Numerically solving Eq. (17) leads to $\alpha \simeq 0.2562$.

each increase α, cause W_f to decrease since $\mathrm{erfc}(x)e^{x^2}$ is a decreasing function of x. Similarly, increasing p_a, which decreases α, causes W_f to increase.

Notice that W_f appears to scale with $(D_a^{(2)})^{1/3}(D_b^{(2)})^{1/6}$ in Eq. (26a), $(D_a^{(2)})^{1/6}(D_b^{(2)})^{1/3}$ in Eq. (26b), and $(D_a^{(2)}D_b^{(2)})^{1/4}$ in Eq. (26c), however, none are true since $D_a^{(2)}$ and $D_b^{(2)}$ are implicit in α. For the case $n=m=1$ we find that $I \simeq 1.902\,50$. A summary of the effects of the various physical

parameters upon the front width are given in Table I for this special case.

D. Product of the reaction

The product of the reaction is now examined. Using Eqs. (17) and (18) to determine α and h, respectively, the outer solution for the product c is then fully specified by Eq. (14). The corresponding concentration profiles are illustrated in Fig. 6. When the product is insoluble in liquid 1, i.e., $p_c=0$ then between the interface and the reaction front, i.e., region 2, the product concentration is a constant equal to h [see Fig. 6(a)]. When the product is more soluble in liquid 1 than in liquid 2, i.e., $p_c>1$, it is possible for the maximum concentration of the product to lie in liquid 1 at the interface and not at the reaction front [see Fig. 6(c)]. This occurs when $p_c[1-(s/\hat{s})\mathrm{erf}(s\alpha)]>1$, which requires that $\mathrm{erf}(s\alpha)<(\hat{s}/s)$. In the cases when the maximum concentration of the product equals h, then we find that increasing $\hat{s}$, s, or ξ leads to an increase in h, whilst increasing p_c leads to a decrease in h. When the maximum concentration of the product occurs in region 1 at the interface then increasing $\hat{s}$, p_c, or ξ leads to an increase in the maximum concentration, whilst there is a nontrivial dependence on s. The effect of the parameters q, p_a, ϕ, ψ, and r upon the maximum concentration is more involved due to their effect on α.

An important quantity is the total amount of product produced which, using Eqs. (14) and (18), is given by $\int_{-\infty}^{\infty} c\,dx = 2\xi e^{-\alpha^2}\sqrt{t}/\{\sqrt{\pi}[q+p_a\,\mathrm{erf}(\alpha)]\}$. Returning to dimensional quantities we have

$$\int_{-\infty}^{\infty} C\,dX = \frac{2k_c^{(2)}A_0\sqrt{D_a^{(2)}}e^{-\alpha^2}\sqrt{T}}{k_a^{(2)}\sqrt{\pi}\left(\sqrt{\dfrac{D_a^{(2)}}{D_a^{(1)}}} + p_a\,\mathrm{erf}(\alpha)\right)}. \qquad (27)$$

We obtain the interesting result that the total amount of product produced in time depends on the ratio $k_c^{(2)}/k_a^{(2)}$ and not on the individual magnitudes of each reaction rate. This in fact does physically make sense since this problem is diffusion limited, i.e., no matter how fast the reaction is it can only consume the reactants inside the reaction zone and the reactants can only enter the reaction zone at their diffusive rates. Thus, given a sufficiently large amount of time even a very slow reaction will enter a diffusion limited state. The center of mass of the product is given by

$$x_c = \frac{\displaystyle\int_{-\infty}^{\infty} xc\,dx}{\displaystyle\int_{-\infty}^{\infty} c\,dx} = \sqrt{t}\left[\alpha + \frac{\hat{s}^2-s^2 p_c}{2s\hat{s}(sp_c+\hat{s})}\sqrt{\pi}\,\mathrm{erfc}(s\alpha)e^{s^2\alpha^2}\right].$$

$$\qquad (28)$$

This quantity can be negative even when $\alpha>0$. Hence, even though we have a reaction front moving to the right (i.e., $\alpha>0$ and $x_f>0$) for immiscible fluids the center of mass of the product can move in the opposite direction ($x_c<0$). This is strikingly different from the miscible case where $x_c=\alpha\sqrt{t}=\frac{1}{2}x_f$, which is equidistant between the position where the

fluids are initially brought into contact and the front position x_f, and hence the center of mass moves along the direction of the reaction front. A useful measure of the width of the product zone, w_c, is obtained from the second moment for c,

$$w_c^2 = \frac{4t}{3}\left[\alpha^2 + \frac{1}{s^2} + \frac{p_c(s^2-\hat{s}^2)}{s\hat{s}^2(sp_c+\hat{s})}\,\text{erfc}(s\alpha)e^{s^2\alpha^2}\right] - x_c^2,$$

(29)

which shows that the width of the product zone scales with $\sqrt{t}$. In particular, for the miscible case, the second moment of the product distribution is $w_c^2=[\alpha^2+(4/s^2)]t/3$. As $\sigma>0$ the product width has a much larger asymptotic limit than the reaction zone width since $w_c \sim \sqrt{t}$ while $w_f \sim t^{(1/2)-\sigma}$.

VI. CONCLUSIONS

The present study has derived analytically the large time asymptotic profiles for the concentrations a, b, and c of reactants A, B, and product C involved in a chemical reaction with effective kinetics $a^n b^m$ when the reactants are each initially contained in immiscible liquids and brought into contact. This study generalizes previous works in miscible systems to cases where the reaction rate for each chemical species can be different and to systems where the two reactants are initially contained in immiscible solvents. Hence the present work provides a unifying framework that allows a treatment of the dynamics both in miscible systems (with the same solvent for A and B) [8,12,18,19] and in immiscible systems. In the case of an immiscible system the problem depends on additional parameters such as the ratio of kinetic constants, the ratio of diffusion coefficients in each fluid, and the partition coefficients. We find that the theoretical scalings [8] already known for miscible fluids are unaltered by the introduction of immiscible fluids.

A parametric study has been conducted showing that for immiscible fluids the speed of the front can be increased by choosing physical parameters favoring transport of the invading species in the invaded fluid, i.e., by increasing its initial concentration, its diffusion coefficient and/or solubility, or by reducing its rate of consumption. On the contrary, the width of the reaction front is increased by increasing the diffusion coefficients inside the invaded fluid or reducing the reaction rates, initial concentrations, the solubility of the invaded fluid, or the diffusion coefficient of the invading species in its initial liquid.

The direction of the front is found to depend on the diffusion coefficient of the invading species in its initial fluid but not on its value in the invading fluid. This has the important consequence that a reaction front in immiscible fluids can travel in the opposite direction to the reaction front formed in miscible fluids for a given fixed range of parameter values. The value of the invading species partition coefficient affects the magnitude of the front speed but it cannot alter the direction of the front. For sufficiently large times, the total amount of product produced in time is independent of the magnitude of the reaction rate. The centre of mass of the product distribution can move in the opposite direction to the first moment of the production rate which is strikingly different to the miscible case.

In summary, the results presented here should allow one to yield insight into the reaction diffusion concentration profiles of systems undergoing a simple effective $A+B\rightarrow C$ reaction in the most general case for both immiscible and miscible systems. Experimental tests of our theoretical predictions could be performed in two-layer systems either in Hele-Shaw cells or in thin tubes. Caution should, however, be taken by using gels or high viscosity solutions to avoid any convective motions which have been shown recently to be able to profoundly affect the dynamics even in horizontal systems [4,7].

APPENDIX A: INNER SOLUTION IN THE REACTION ZONE

The solution in the outer region was obtained by vanishing both reactants at the point $x=x_f(t)$, effectively considering an infinitely thin reaction zone. However, the reaction zone is a small region in which a and b overlap. Note that without an overlap region the term $a^n b^m$ would be identically zero everywhere. The reaction-diffusion equations at the reaction front are given by Eqs. (7d)–(7f) for liquid 2 defined for regions 2 and 3, namely,

$$a_t = a_{xx} - a^n b^m, \quad b_t = \frac{b_{xx}}{r^2} - \psi a^n b^m, \quad c_t = \frac{c_{xx}}{s^2} + \xi a^n b^m.$$

(A1)

In order to examine this inner region we introduce the inner coordinate

$$Z = (\eta - \alpha)t^\sigma,$$

(A2)

where $\sigma>0$ so that as t tends to infinity the term Z/t^σ tends to zero corresponding to η tending to α. Expanding the outer region solutions (14) around $\eta=\alpha$, i.e., around the front and substituting $(\eta-\alpha)=Z/t^\sigma$ we obtain, to leading order

$$a^{(2)} \rightarrow -\frac{UZ}{t^\sigma}, \quad b^{(2)} \rightarrow 0, \quad c^{(2)} \rightarrow h\left(1+\frac{W_L Z}{t^\sigma}\right),$$

(A3a)

$$a^{(3)} \rightarrow 0, \quad b^{(3)} \rightarrow \frac{VZ}{t^\sigma}, \quad c^{(3)} \rightarrow h\left(1-\frac{W_R Z}{t^\sigma}\right),$$ (A3b)

where

$$U = \frac{2e^{-\alpha^2}}{\sqrt{\pi}[q+p_a\,\text{erf}(\alpha)]}, \quad V = \frac{2\phi r e^{-r^2\alpha^2}}{\sqrt{\pi}\,\text{erfc}(r\alpha)}, \quad \text{(A3c)}$$

$$W_L = \frac{2s^2 p_c e^{-s^2 \alpha^2}}{\sqrt{\pi}[\hat{s} + s p_c \, \mathrm{erf}(s\alpha)]}, \quad W_R = \frac{2s e^{-s^2 \alpha^2}}{\sqrt{\pi} \, \mathrm{erfc}(s\alpha)}.$$

(A3d)

We now seek an inner solution (a_I, b_I, c_I) in a form that can match the outer solution by writing

$$a_I = \frac{\mathcal{A}(Z)}{t^\sigma}, \quad b_I = \frac{\mathcal{B}(Z)}{t^\sigma}, \quad c_I = h + \frac{\mathcal{C}(Z)}{t^\sigma}, \quad (A4)$$

so that for large times the inner solutions for a and b tend to zero whilst c tends to a finite value h [see Eqs. (A3)]. Inserting Eq. (A4) into Eq. (A1) using Eq. (A2) we get

$$\frac{\sigma \mathcal{A}}{t^{2\sigma}} + \left[(1 - 2\sigma)\frac{Z}{t^{2\sigma}} + \frac{\alpha}{t^\sigma} \right] \frac{\mathcal{A}_Z}{2} + \frac{\mathcal{A}_{ZZ}}{4} = \frac{\mathcal{A}^n \mathcal{B}^m}{t^{(1+n+m)\sigma - 1}},$$

$$\frac{\sigma \mathcal{B}}{t^{2\sigma}} + \left[(1 - 2\sigma)\frac{Z}{t^{2\sigma}} + \frac{\alpha}{t^\sigma} \right] \frac{\mathcal{B}_Z}{2} + \frac{\mathcal{B}_{ZZ}}{4r^2} = \frac{\psi \mathcal{A}^n \mathcal{B}^m}{t^{(1+n+m)\sigma - 1}},$$

$$\frac{\sigma \mathcal{C}}{t^{2\sigma}} + \left[(1 - 2\sigma)\frac{Z}{t^{2\sigma}} + \frac{\alpha}{t^\sigma} \right] \frac{\mathcal{C}_Z}{2} + \frac{\mathcal{C}_{ZZ}}{4s^2} = -\frac{\xi \mathcal{A}^n \mathcal{B}^m}{t^{(1+n+m)\sigma - 1}}.$$

We notice that in these equations the powers of t present are -2σ, $-\sigma$, 0, and $1 - (1 + n + m)\sigma$. As t tends to infinity, with $\sigma > 0$, a balance of the $\mathcal{O}(1)$ terms requires

$$\sigma = \frac{1}{1 + n + m}, \quad (A5)$$

which is the same scaling first determined by Cornell *et al.* [8]. The leading order terms require that

$$\mathcal{A}_{ZZ} = \frac{\mathcal{B}_{ZZ}}{\psi r^2} = -\frac{\mathcal{C}_{ZZ}}{\xi s^2} = 4\mathcal{A}^n \mathcal{B}^m. \quad (A6)$$

Solving the equations in Eqs. (A6) along with suitable boundary conditions provides the functions $\mathcal{A}(Z)$, $\mathcal{B}(Z)$, and $\mathcal{C}(Z)$ that define the inner solution (A4).

APPENDIX B: MATCHING INNER AND OUTER SOLUTIONS

The analytical solution (14) in the outer region was found and depends on two unknown constants h and α. The matching conditions for the inner solution (A4) with the left and right outer solutions (A3) are

$$\mathcal{A} \to -UZ, \quad \mathcal{B} \to 0, \quad \mathcal{C} \to h W_L Z \quad \text{as } Z \to -\infty,$$

(B1a)

$$\mathcal{A} \to 0, \quad \mathcal{B} \to VZ, \quad \mathcal{C} \to -h W_R Z \quad \text{as } Z \to \infty.$$

(B1b)

The linear equations in Eqs. (A6) are $\mathcal{A}_{ZZ} = \mathcal{B}_{ZZ}/(\psi r^2) = -\mathcal{C}_{ZZ}/(\xi s^2)$ which can be integrated twice and after using the matching conditions as $Z \to -\infty$ we obtain

$$\mathcal{A} + UZ = \frac{\mathcal{B}}{\psi r^2} = -\frac{\mathcal{C}}{\xi s^2} + \frac{h W_L}{\xi s^2} Z.$$

The matching conditions as $Z \to \infty$ yield two conditions, namely,

$$h = \frac{U \xi s^2}{W_R + W_L} \quad \text{and} \quad V = U \psi r^2. \quad (B2)$$

These conditions are equivalent to Eqs. (17) and (18). Using Eq. (B2) we can express $\mathcal{B}$ and $\mathcal{C}$ as

$$\mathcal{B} = V\left(\frac{\mathcal{A}}{U} + Z\right), \quad \mathcal{C} = -\xi s^2\left(\mathcal{A} + \frac{W_R UZ}{W_R + W_L}\right). \quad (B3)$$

Thus $\mathcal{A}$ is determined from the ordinary differential equation

$$\mathcal{A}_{ZZ} = 4V^m \mathcal{A}^n (Z + \mathcal{A}/U)^m$$

under the two constraints that

$$\mathcal{A} \to -UZ \quad \text{as } Z \to -\infty \quad \text{and} \quad \mathcal{A} \to 0 \quad \text{as } Z \to \infty.$$

By scaling $Z = z/\lambda$ and

$$\mathcal{A} = \frac{UG}{\lambda}, \quad (B4)$$

we obtain

$$G_{zz} = G^n (G + z)^m, \quad (B5a)$$

where $\lambda = (4V^m U^{n-1})^\sigma$. The far field conditions become

$$G \to -z \quad \text{as } z \to -\infty \quad \text{and} \quad G \to 0 \quad \text{as } z \to \infty.$$

(B5b)

This system is identical to system (27) obtained by Magnin [10] who analyzed this problem when the diffusion coefficients are equal. Analytical solutions for the inner solution G have not been found, hence numerics have to be employed to solve system (B5a) and (B5b). Notice that, when $n = m$, we have $G(-z) \equiv G(z) + z$, thus $G_z(0) = -\frac{1}{2}$ and $G_{zzz}(0) = 0$ so that G_{zz} is maximum at $z = 0$. Thus, in this special case the position of the front can be considered as the point where the rate of reaction has its maximum.

APPENDIX C: POSITION x_f AND WIDTH w_f OF THE REACTION FRONT

Appendixes A and B explicitly allow the rate of production $R = \xi a_I^n b_I^m$ to be expressed. Indeed using Eq. (A4) with $\mathcal{A}$ and $\mathcal{B}$ given by Eqs. (B4) and (B3), respectively, we get

$$R = \frac{1}{4} \xi U \lambda t^{-(n+m)\sigma} G_{zz},$$

where the function G depends on n and m and the term $U\lambda$ depends on ψ, r, q, ϕ, p_a, n and m, respectively. The time scaling is the most dominant factor revealing that smaller values of n and m yield larger reaction rates for a given t. Using the coordinate scaling $dx = 2\lambda^{-1} t^{(1/2) - \sigma} dz$ allows the following integrals to be evaluated:

$$\int_{-\infty}^{\infty} R \, dx = \frac{\xi U}{2\sqrt{t}} \int_{-\infty}^{\infty} G_{zz} \, dz = \frac{\xi U}{2\sqrt{t}},$$

$$\int_{-\infty}^{\infty} Rx\,dx = \xi U \int_{-\infty}^{\infty} G_{zz}\left(\alpha + \frac{z}{\lambda t^{\sigma}}\right)dz = \xi U \alpha,$$

where the results $\int_{-\infty}^{\infty} G_{zz}dz = [G_z]_{-\infty}^{\infty} = 1$ and $\int_{-\infty}^{\infty} zG_{zz}dz = [zG_z - G]_{-\infty}^{\infty} = 0$ have been utilized. Thus, the first moment of R is given by

$$\frac{\displaystyle\int_{-\infty}^{\infty} xR\,dx}{\displaystyle\int_{-\infty}^{\infty} R\,dx} = 2\alpha\sqrt{t} \equiv x_f. \tag{C1}$$

Hence, the first moment of the reaction rate is equivalent to the position of the reaction front x_f given by Eq. (12).

The second moment of the production rate is a useful measure of the size of the reaction front, w_f. Consider

$$\int_{-\infty}^{\infty} R(x - x_f)^2 dx = \frac{2\xi U}{\lambda^2} t^{(1/2)-2\sigma} I, \quad I = \int_{-\infty}^{\infty} G_{zz}z^2 dz,$$

where the integral I must be evaluated numerically since there is no analytical solution for G. Introducing the notation I_{nm}, where the subscripts n and m denote their values, we find that $I_{11} \simeq 1.902\,50$, $I_{12} = I_{21} \simeq 3.296\,68$, and $I_{22} \simeq 3.761\,55$. Using Eq. (6) we obtain

$$w_f = \frac{2\sqrt{I}}{\lambda} t^{(1/2)-\sigma}, \tag{C2}$$

illustrating that the reaction front width scales with $t^{(1/2)-\sigma}$,

[1] K. Eckert and A. Grahn, Phys. Rev. Lett. **82**, 4436 (1999).
[2] K. Eckert, M. Acker, and Y. Shi, Phys. Fluids **16**, 385 (2004).
[3] D. A. Bratsun, Y. Shi, K. Eckert, and A. De Wit, Europhys. Lett. **69**, 746 (2005).
[4] Y. Shi and K. Eckert, Chem. Eng. Sci. **61**, 5523 (2006).
[5] Y. Shi and K. Eckert, Chin. J. Chem. Eng. **15**, 748 (2007).
[6] O. Citri, M. L. Kagan, R. Kosloff, and D. Avnir, Langmuir **6**, 3 (1990).
[7] L. Rongy, P. M. J. Trevelyan, and A. De Wit, Phys. Rev. Lett. **101**, 084503 (2008).
[8] S. Cornell, M. Droz, and B. Chopard, Phys. Rev. A **44**, 4826 (1991).
[9] S. Cornell, Z. Koza, and M. Droz, Phys. Rev. E **52**, 3500 (1995).
[10] J. Magnin, Eur. Phys. J. B **17**, 673 (2000).
[11] B. Chopard, M. Droz, J. Magnin, and Z. Rácz, Phys. Rev. E **56**, 5343 (1997).
[12] L. Gálfi and Z. Rácz, Phys. Rev. A **38**, 3151 (1988).
[13] G. Venzl, J. Chem. Phys. **85**, 2006 (1986).
[14] Y.-E. L. Koo and R. Kopelman, J. Stat. Phys. **65**, 893 (1991).
[15] A. Yen and R. Kopelman, Phys. Rev. E **56**, 3694 (1997).
[16] H. Taitelbaum, Yong-Eun Lee Koo, S. Havlin, R. Kopelman, and G. H. Weiss, Phys. Rev. A **46**, 2151 (1992).
[17] S. Cornell and M. Droz, Phys. Rev. Lett. **70**, 3824 (1993).
[18] Z. Koza, J. Stat. Phys. **85**, 179 (1996).
[19] M. Sinder and J. Pelleg, Phys. Rev. E **62**, 3340 (2000).
[20] P. W. Atkins, *Physical Chemistry*, 6th ed. (Oxford University Press, New York, 1997).
[21] P. Polanowski and Z. Koza, Phys. Rev. E **74**, 036103 (2006).
[22] S. H. Park, H. Peng, R. Kopelman, and H. Taitelbaum, Phys. Rev. E **75**, 026107 (2007).
[23] J. Crank, *The Mathematics of Diffusion*, 2nd ed. (Oxford University Press, New York, 1975).
[24] H. S. Carslaw and J. C. Jaeger, *Conduction of Heat in Solids*, 2nd ed. (Clarendon, Oxford, 1959).
[25] Z. Jiang and C. Ebner, Phys. Rev. A **42**, 7483 (1990).